Check for updates

Received: 6 February 2022 | Revised: 5 June 2022 | Accepted: 10 June 2022

DOI: 10.1002/hbm.25992

RESEARCH ARTICLE

WILEY

Pain-related reorganization in the primary somatosensory cortex of patients with postherpetic neuralgia

Hong Li[1,2] | Xiaoyun Li[2,3] | Jiyuan Wang[1,2] | Fei Gao[4] | Katja Wiech[5] | Li Hu[2,3] | Yazhuo Kong[1,2,5]

[1]CAS Key Laboratory of Behavioral Science, Institute of Psychology, Beijing, China

[2]Department of Psychology, University of Chinese Academy of Sciences, Beijing, China

[3]CAS Key Laboratory of Mental Health, Institute of Psychology, Beijing, China

[4]Department of Pain Medicine, Peking University People's Hospital, Beijing, China

[5]Wellcome Centre for Integrative Neuroimaging (WIN), Nuffield Department of Clinical Neurosciences, University of Oxford, John Radcliffe Hospital, Oxford, UK

Correspondence

Li Hu, Key Laboratory of Mental Health, Institute of Psychology, Chinese Academy of Sciences, Beijing, China, 100101.
Email: huli@psych.ac.cn

Yazhuo Kong, Key Laboratory of Behavioral Science, Institute of Psychology, Chinese Academy of Sciences, Beijing, China, 100101.
Email: kongyz@psych.ac.cn

Funding information

National Natural Science Foundation of China, Grant/Award Numbers: 81871436, 31671141, 31822025, 82072010, 82101610

Abstract

Studies on functional and structural changes in the primary somatosensory cortex (S1) have provided important insights into neural mechanisms underlying several chronic pain conditions. However, the role of S1 plasticity in postherpetic neuralgia (PHN) remains elusive. Combining psychophysics and magnetic resonance imaging (MRI), we investigated whether pain in PHN patients is linked to S1 reorganization as compared with healthy controls. Results from voxel-based morphometry showed no structural differences between groups. To characterize functional plasticity, we compared S1 responses to noxious laser stimuli of a fixed intensity between both groups and assessed the relationship between S1 activation and spontaneous pain in PHN patients. Although the intensity of evoked pain was comparable in both groups, PHN patients exhibited greater activation in S1 ipsilateral to the stimulated hand. Pain-related activity was identified in contralateral superior S1 (SS1) in controls as expected, but in bilateral inferior S1 (IS1) in PHN patients with no overlap between SS1 and IS1. Contralateral SS1 engaged during evoked pain in controls encoded spontaneous pain in patients, suggesting functional S1 reorganization in PHN. Resting-state fMRI data showed decreased functional connectivity between left and right SS1 in PHN patients, which scaled with the intensity of spontaneous pain. Finally, multivariate pattern analyses (MVPA) demonstrated that BOLD activity and resting-state functional connectivity of S1 predicted within-subject variations of evoked and spontaneous pain intensities across groups. In summary, functional reorganization in S1 might play a key role in chronic pain related to PHN and could be a potential treatment target in this patient group.

KEYWORDS

functional magnetic resonance imaging, pain perception, postherpetic neuralgia, primary somatosensory cortex (S1), reorganization

This is an open access article under the terms of the Creative Commons Attribution-NonCommercial-NoDerivs License, which permits use and distribution in any medium, provided the original work is properly cited, the use is non-commercial and no modifications or adaptations are made.
© 2022 The Authors. *Human Brain Mapping* published by Wiley Periodicals LLC.

1 | INTRODUCTION

In the context of pain, multiple brain regions, such as the anterior cingulate cortex (ACC), insula cortex, and the primary and secondary somatosensory cortices (S1 and S2) are involved in the complex experiences of pain. Nevertheless, the role of different cortical areas in pain processing is controversial, particularly that of S1 (Apkarian et al., 2005; Hu et al., 2015; Valentini et al., 2012).

Experimental studies in animals and humans suggest that maladaptive changes in S1 are a feature of neuropathic pain (Seifert & Maihofner, 2009). For example, Endo et al. demonstrated that mechanical hypersensitivity is associated with heightened contralateral S1 activity in an experimental model of neuropathic pain in rats (Endo et al., 2008). In humans, studies using fMRI and positron emission tomography (PET) have demonstrated increased S1 responses to innocuous and noxious peripheral stimulation in patients with chronic pain, such as fibromyalgia and phantom limb pain (PLP) (Bjorkman et al., 2012; Desbordes et al., 2015).

In addition to S1 hyperexcitability, changes in its somatotopic organization through altered afferent input have been linked to pain chronification, and have mainly been investigated for PLP (Flor et al., 1995; Makin et al., 2013), complex regional pain syndrome (CRPS), and spinal cord injury (SCI). In CRPS patients, Juottonen et al. (2002) found a shortened distance between thumb and little finger representations in the S1 corresponding to the affected hand (Juottonen et al., 2002). Maihofner et al. (2003) observed that the S1 representation of the center of the hand moved toward that of the lip in CRPS patients, and this cortical reorganization scaled with the degree of CRPS pain and the extent of mechanical hyperalgesia (Maihofner et al., 2003). A close relationship between the progressive atrophic as well as microstructural reorganization across the somatosensory cortex and the sensory outcome following SCI has been described (Freund et al., 2011; Grabher et al., 2015; Kambi et al., 2014).

Postherpetic neuralgia (PHN), which is defined as pain persisting for more than three months following the onset or healing of herpes zoster, is one of the most common types of chronic peripheral neuropathic pain (Scholz, Finnerup et al., 2019). PHN-related pain comprises spontaneous pain (e.g., sharp, burning, and aching) as well as dynamic mechanical allodynia. Patients suffering from PHN often exhibit multiple signs of peripheral and central neuropathy (e.g., hyperalgesia, allodynia, and sensory loss) as well as cerebral alterations in multiple brain regions, including S1 (Dworkin, 2002; Geha et al., 2007; Price, 2000; Sah et al., 2003). Importantly, spontaneous pain in PHN patients was directly linked to increased cerebral blood flow (CBF) in the S1 (Liu et al., 2013; Liu et al., 2017). However, whether the perception of evoked and spontaneous pain related to PHN involves structural or functional S1 reorganization has not explicitly been addressed.

In this study, we explored (1) S1 activity and functional organization related to evoked pain in PHN patients and healthy controls and (2) related to spontaneous pain in the patient group. Furthermore, we investigated (3) whether bilateral S1 resting-state functional connectivity in PHN patients could be related to the intensity of chronic pain. Lastly, we used a multivariate pattern analysis (MVPA) approach to test (4) whether structural and functional features of S1 can predict laser-evoked and spontaneous pain intensities across PHN patients and healthy controls. Among the cortical regions frequently activated by pain are S1 and S2, and a growing number of researchers believe that neuropathic pain is consistently associated with S1 functional plasticity. Previous reports led us to hypothesize that the PHN is associated with regional S1 functional and structural plasticity changes and the degree of plasticity is highly correlated to pain intensity; and then, chronic pain may prompt that person to developing changes in the activity of pain-encoding areas.

2 | MATERIALS AND METHODS

2.1 | Participants

Sixteen right-handed PHN patients (5 males; mean age = 65.75 years; SD = 6.99) and 20 age- and gender-matched right-handed healthy controls (HC, 8 males; Mean age = 61.55 years; SD = 8.21) participated in the study. Patients fulfilled the International Association for the Study of Pain (IASP) criteria for PHN and were diagnosed by experienced clinicians based on clinical symptoms (including medical history, shingles history, pain severity, and pain types; Fields et al., 1998). Characteristics of patients with PHN are shown in Table S1. On average, PHN patients reported a spontaneous pain intensity of 3.06 ± 1.28 (present pain intensity, PPI; mean ± SD), with an average duration of 2.42 ± 3.36 years. All PHN patients were requested to stop taking any analgesic medication 1 week before the MRI scan. None of the participants had a past or current diagnosis of any psychiatric or major neurological illness. The study was run in accordance with the Declaration of Helsinki, and the Ethics Committee at the Institute of Psychology, Chinese Academy of Sciences, approved the study (the National Natural Science Foundation of China, No: 31671141). Written informed consent was obtained from all participants before enrolling in the study.

2.2 | Demographic and pain characteristics

All participants provided demographic information (age, gender, and educational level) and completed psychological questionnaires to assess depression (Beck's Depression Index, BDI) (Beck et al., 1996) as well as state and trait anxiety (State–Trait Anxiety Index, STAI). Spontaneous pain was assessed using the short form of the McGill Pain Questionnaire (SF-MPQ) (Melzack, 1987). The SF-MPQ contains (1) a pain rating index (PRI), which consists of 15 descriptors ranging from 0 (none) to 3 (severe); (2) a present pain intensity (PPI) index ranging from 0 (no pain) to 5 (unbearable pain); (3) a 10-cm visual analogue scale (VAS) to assess the intensity of the mean daily pain during the past 2 weeks. The SF-MPQ total score is the sum of the three indices.

2.3 | Experimental design

The experiment comprised three different MRI scans in a fixed order: a T1-weighted structural scan, a resting-state fMRI scan, and a task fMRI scan. A schematic overview of the paradigm is shown in Figure 1a. For the resting-state fMRI scan, participants were required to lay supine in the scanner and keep their eyes fixed on a white cross centered on the screen for 10 min. For the task fMRI scan, 20 nociceptive stimuli were delivered to a square area on the dorsum of the left hand (see details below). Each trial started with a 6s fixation of a white cross centered on the screen, followed by the delivery of a nociceptive stimulus with a duration of 4 ms. A visual cue was presented 15 s after the nociceptive stimulus to prompt participants to rate the pain intensity and unpleasantness on an 11-point Visual Analog Scale (VAS), with 0 indicating "no sensation" and 10 indicating "unbearable sensation" within 6 s by pressing buttons on a shank in their right hand (Figure 1b). The inter-trial interval (ITI) varied randomly between 1 and 2 s.

2.4 | Nociceptive stimuli

Nociceptive stimuli were pulses of radiant heat generated by an infrared neodymium yttrium aluminum perovskite (Nd:YAP) laser with a wavelength of 1.34 μm (Electronic Engineering, Florence, Italy). We decided to use noxious laser stimuli as they specifically activate $A\delta$ fiber and avoid the potentially confounding effect of touch from contact with skin. Moreover, laser stimuli are short-lasting and safe to apply, which enabled us to acquire laser-evoked brain activation quickly in the fMRI experiment. Laser pulses were delivered to a circular area (diameter ≈4 cm) on the dorsum of the participant's left hand. The laser beam was set at a diameter of ∼7 mm by focusing lenses connected to the optic fiber, with a fixed stimulus intensity of 3.5 J to elicit a painful pinprick sensation (Bromm & Treede, 1984). To prevent nociceptor fatigue or sensitization, the laser beam target was manually shifted by about 1 cm in a random direction after each stimulus (Jin et al., 2018). Notably, we only applied nociceptive stimuli to the participants' left hand and expected to obtain brain activation in the contralateral S1.

2.5 | MRI data acquisition

Both structural and functional MRI data were acquired on a 3.0 T GE-MRI scanner with an 8-channel head coil at the Institute of Psychology, Chinese Academy of Sciences. For each participant, a T1-weighted structural image was acquired using a 3D SPGR sequence (TR/TE = 6.9/2.9 ms, FA = 8°, FOV = 256 mm × 256 mm, matrix = 256 × 256, slices = 192, slice thickness = 1.0 mm). A whole-brain gradient-echo, echo-planar imaging (GE-EPI) sequence was used to obtain functional data with 300 volumes for resting-state fMRI scan (TR/TE = 2000/30 ms; flip angle: 90°; FOV = 220 mm × 220 mm; matrix = 64 × 64; slice thickness = 4 mm; slices = 30) and 320 volumes for the task fMRI scan (TR/TE = 2000/30 ms; flip angle: 70°; FOV = 220 mm × 220 mm; matrix = 64 × 64; slice thickness = 3 mm; slices = 43).

2.6 | Voxel-based morphometry

Gray matter volume was examined using voxel-based morphometry from FSLVBM. Voxel-based morphometry (VBM) has been used for identifying gray matter volume (GMV) changes in diseases with chronic pain such as the trigeminal neuralgia, fibromyalgia, and chronic back pain (Li et al., 2017; Luerding et al., 2008; May, 2011; Obermann et al., 2013). In our study, we selected the VBM is to allow for comparisons with studies on other types of neuropathic pain which have mainly focused on S1 and VBM. All T1-weighted images were first brain extracted and then segmented into gray matter, white matter, or cerebrospinal fluid. A gray matter template was generated by registering and averaging all gray matter images. The gray matter image for each participant was then registered to the template using non-linear transformation. A voxel-wise permutation test was used to identify significant group differences between PHN patients and HC to a distribution generated from 5000 permutations of the data for each voxel of the template, using a sigma filter of 3 mm for smoothing. The $p < .05$ (FWE, using the Threshold-Free Cluster Enhancement [TFCE] method) were considered statistically significant.

2.7 | fMRI data pre-processing

The fMRI image processing and data analyses were performed using FMRI Expert Analysis Tool (FEAT), version 5.98, which is part of the Functional Magnetic Resonance Imaging of the Brain (FMRIB) Software Library (FSL; http://www.fmrib.ox.ac.uk/fsl/). Pre-processing of functional imaging data included motion correction using MCFLIRT (Jenkinson et al., 2002); removal of non-brain structures using Brain Extraction Tool (Smith et al., 2002); spatial smoothing using a Gaussian kernel with a 5-mm FWHM, and high-pass temporal filtering (cut-off: 100 s). Independent component analysis (ICA)-based denoising was performed (Beckmann & Smith, 2004) for each individual fMRI data to remove the artifacts, including head motion, white matter and cerebrospinal fluid noise, high-frequency noise, slice dropouts, gradient instability, EPI ghosting, and field inhomogeneities.

2.8 | Task fMRI: General linear model analysis

Task fMRI data was modeled on a voxel-by-voxel basis using a general linear model (GLM) approach (Woolrich et al., 2001), and a whole-brain analysis as well as S1-specific ROI analyses, were conducted. The fMRI time series were modeled using a series of regressors, including the events of interest (i.e., the occurrence of laser stimuli, rating period) convolved with a gamma hemodynamic response function and their temporal derivatives. For each individual, parameter estimates for the regressors that described BOLD activation evoked

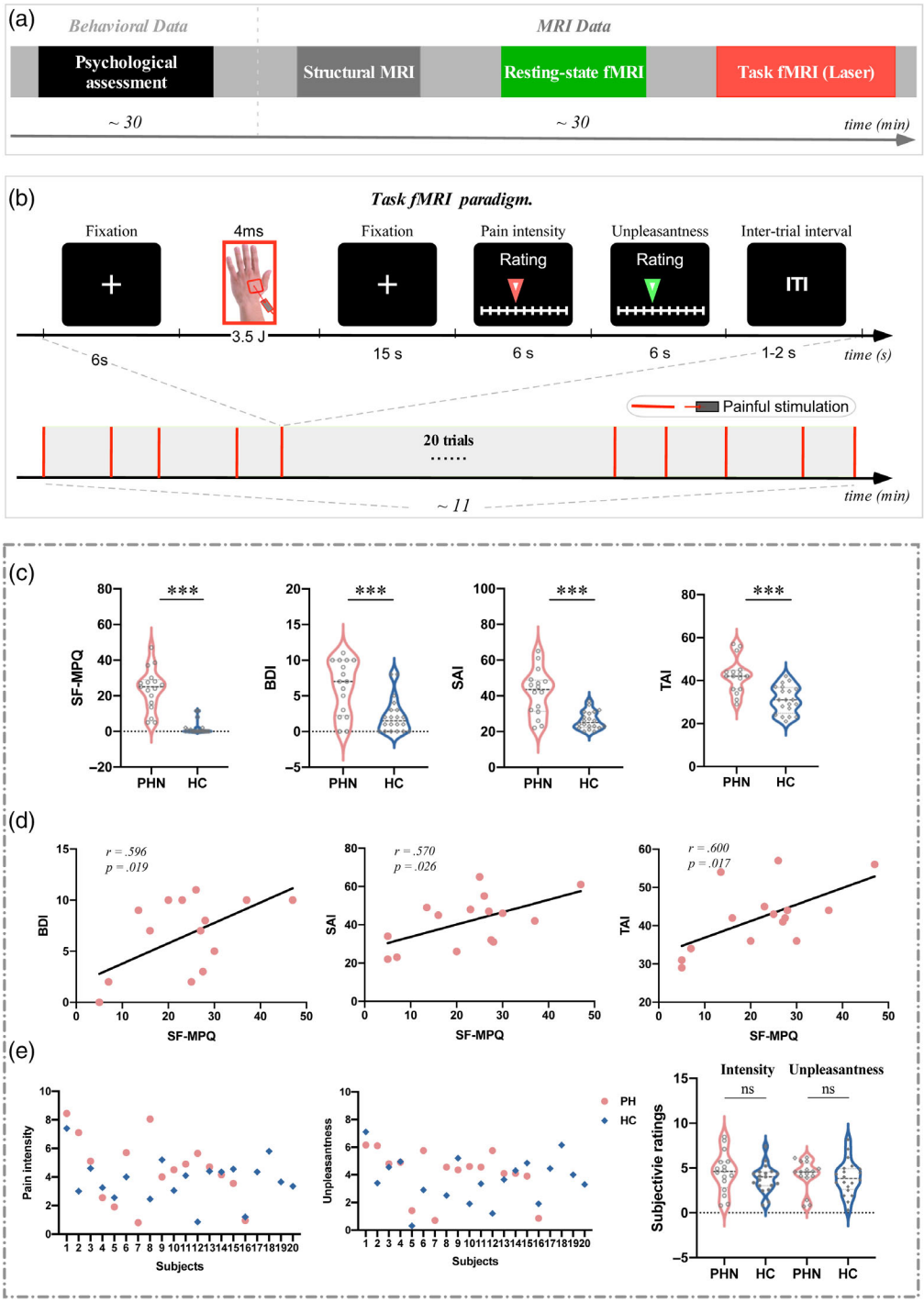

FIGURE 1 Experimental paradigms and pain characteristics. (a) a schematic diagram summarizing the experimental design. Participants' pain characteristics were confirmed during a psychological assessment. The MRI data consisted of three different scans: Scan 1 = high-resolution structural scan; scan 2 = resting-state functional MRI data were acquired; scan 3 = task functional MRI data were acquired during nociceptive laser stimuli applied to the participants' dorsum of the left hand. Each scan is represented visually by a different color. (b) Design of task fMRI paradigm, which contained a single block of 20 trials with transient laser stimuli. Each trial started with a 6s fixation of the white cross centered on the screen and followed by the delivery of a nociceptive stimulus. A visual cue presented 15 s after the nociceptive stimulus prompted the participants to rate the perceived intensity and unpleasantness within 6 s on the 11-point NRS, respectively. The inter-trial interval (ITI) was 1–2 s. (c) The comparison of pain intensities (SF-MPQ) and psychological variables (i.e., BDI, SAI, and TAI) between PHN patients and HC. Pain intensity ratings (SF-MPQ) and psychological variables (i.e., BDI, SAI, and TAI) were significantly larger in PHN patients than in HC (***$p < .001$). (d) The correlation between pain intensities and psychological variables in PHN patients. SF-MPQ ratings were positively correlated with BDI, SAI, and TAI scores in PHN patients. (e) Scatter plots of perceived intensity and unpleasantness of nociceptive stimuli for all individuals, and the comparison of pain intensity and unpleasantness between PHN patients and HC. The perceived intensity and unpleasantness to nociceptive stimuli were not significantly different between PHN patients and HC (ns, not significant). BDI, Beck-depression index; SAI, state-anxiety index; SF-MPQ, short-form McGill pain questionnaire; TAI, trait-anxiety index.

by the laser stimuli were generated. The contrast of parameter estimates (COPE) images was co-registered to a standard template in a two-stage spatial registration process: fMRI to structural images using FMRIB's Linear Image Registration Tool (FLIRT) (Jenkinson et al., 2002) and structural images to a standard template (MNI152-2 mm) using FMRIB's Non-linear Image Registration Tool (FNIRT). Group-level statistical analyses (group average and difference) were carried out using a mixed-effect approach (FLAME, FMRIB's Local Analysis of Mixed Effects; Beckmann et al., 2003; Woolrich et al., 2004) with one-sample *t*-tests to obtain mean brain responses to nociceptive stimuli for each group and independent sample *t*-test to compare responses between groups. To test for differences in stimulus-evoked S1 activity between PHN patients and HC, BOLD activity was compared between both groups using a region-of-interest approach with unilateral S1 defined in MNI space based on the Harvard–Oxford atlas (90% thresholded). Thus, we defined a new variable HEMISPHERE (ipsilateral [$S1_{Left}$] and contralateral [$S1_{Right}$] side corresponding to the stimulation site). We performed a two-way analysis of variance (ANOVA) with a between-subject factor GROUP (PHN vs. HC) and a within-subject factor HEMISPHERE ($S1_{Left}$ vs. $S1_{Right}$). If the interaction between the two factors was significant, post-hoc paired sample *t*-tests were carried out to compare $S1_{Left}$ and $S1_{Right}$ activity, separately for PHN patients and HC. Bonferroni correction was applied for multiple comparisons. In addition, we also examined brain responses associated with laser-evoked pain and spontaneous pain in PHN patients. A general linear model was used with pain ratings for laser-evoked pain as regressors of interest and age, gender, and pain durations as covariates to determine pain-related activation across the whole brain. The SF-MPQ questionnaire (Melzack, 1987) was used to assess the intensity of spontaneous pain. Pain intensities were demeaned (zeroing set to mean) and included as regressors to determine their relationships to brain activity after controlling the effects of age, gender, and pain durations. Statistical images for activations of laser-evoked pain were thresholded using cluster-forming correction determined by $z > 2.3$ and a corrected cluster significance threshold of $p < .05$. Activity during spontaneous pain was analyzed using FSL-*Randomize* with 5000 permutations within the S1 mask ($p < .05$ TFCE corrected). As explained in more detail in the Section 3, our analyses of laser-evoked and spontaneous pain in PHN patients revealed different activation patterns in the inferior and superior portions of S1. To follow up on these findings, we divided the S1 mask into an inferior (IS1) and a superior portion (SS1) in MNI space based on the encoding regions from the task fMRI results for further resting-state functional connectivity analyses (cortical coordinates in both hemispheres: $z = 56$).

2.9 | Resting-state fMRI: Seed-based functional connectivity analysis

As our analyses of laser-evoked and spontaneous pain in PHN patients revealed different encoding patterns in IS1 and SS1, we decided to compare resting-state functional connectivity between both groups separately for bilateral IS1 and bilateral SS1. The same S1 ROIs as defined in the section on task-fMRI were used in the resting-state analysis. First, IS1 and SS1 masks were registered back into each participant's native space. Next, we extracted the BOLD time series from the seed regions and subsequently calculated the correlations between the bilateral IS1 as well as bilateral SS1 while controlling for participants' age, gender, and the duration of pain in both groups. The resulting correlation coefficients were converted to *z* scores for further statistical analysis. Independent sample *t*-tests were used for each ROI to detect differences between PHN patients and HC. Pearson correlation analyses were performed to assess the relationship between pain intensities and functional connectivity in PHN patients. In order to explore the specificity of our S1 findings, the same connectivity analysis was performed for the left and right primary motor cortex (M1). We chose M1 as the control region because it is located adjacent to S1 in the parietal cortex but subserves a very different function.

2.10 | Multivariate pattern analysis

Multivariate pattern analysis (MVPA) was used to investigate whether structural and functional features of S1 ROIs (IS1 and SS1), as defined above, were able to predict evoked pain in HC and spontaneous as well as evoked pain in PHN patients. The relationship between the extracted BOLD signals/gray matter volume and spontaneous/evoked pain ratings in PHN patients and HC were modeled using a multivariate linear regression (MVLR) and decoded using a support vector regression (SVR), as implemented in the LIBSVM toolbox. The calculation resulted in a pattern of prediction weights for all independent variables (Tu et al., 2019). The prediction of pain ratings was achieved based on the leave-one-subject-out cross-validation procedure. In each iteration, data of one participant was selected as the test sample, and datasets of the remaining participants were used as training samples. This procedure was repeated until data of each participant had been used as the test sample once. The predicted pain rating was calculated by taking the dot product of the pattern of prediction weights obtained from the training samples and the BOLD signals/gray matter volume in S1 ROIs from the test sample. To evaluate the prediction performance, we calculated the prediction–outcome correlation, which was defined as the correlation coefficient between the actual and predicted magnitudes of pain rating (Doehrmann et al., 2013; Lindquist et al., 2017; Wager et al., 2011). We also examined whether resting-state functional connectivity of bilateral S1 ROIs was able to predict spontaneous pain ratings (SF-MPQ ratings) in PHN patients. The prediction was modeled using the same MVLR and decoded using the same SVR as described above.

2.11 | Statistical analysis

Independent sample *t*-tests were used for detecting differences in demographic, pain, psychological variables, and mean pain intensity

ratings following laser stimulation between PHN patients and HC. For PHN patients, Pearson correlation analyses were performed to assess the relationship between pain intensities and psychological variables. The significance level was set as $p < .05$.

3 | RESULTS

3.1 | Psychophysics

The comparison of demographic, pain, and psychological characteristics between PHN patients and HC is summarized in Table 1. The two groups did not differ significantly with respect to gender, age, and education level. As expected, the intensity of pain, as quantified by PRI, PPI, VAS, and total SF-MPQ scores were significantly higher in PHN patients than in HC (Table 1, Figure 1c). In addition, patients reported higher levels of depression as well as state and trait anxiety (Table 1, Figure 1c).

In PHN patients, BDI, SAI, and TAI scores were all positively correlated with SF-MPQ total scores (BDI vs. SF-MPQ: $r = .596$, $p = .019$; SAI vs. SF-MPQ: $r = .570$, $p = .026$; TAI vs. SF-MPQ: $r = .600$, $p = .017$; Figure 1d).

Scatter plots of the perceived intensity and unpleasantness of noxious laser stimuli for all participants are shown in Figure 1e. Mean perceived intensity ($t[34] = 0.621$, $p = .539$) and unpleasantness ($t[34] = 0.412$, $p = .683$) of pain were not significantly different between PHN patients and HC, which indicates that the nociceptive laser stimuli of a fixed stimulation intensity induced a comparable sensation in both groups (Figure 1e).

3.2 | Voxel-based morphometry analysis

The whole-brain VBM analysis did not reveal any significant differences in gray matter volume between PHN patients and HC, indicating that PHN was not linked to evident structural changes in our sample. We also found no significant group differences when the analysis was limited to S1 (region-of-interest analysis).

3.3 | BOLD activations in response to nociceptive laser stimuli in S1

Stimulus-locked noxious laser stimuli elicited significant activation in a wide range of pain-associated brain regions in both PHN patients (Figure 2a, top panel) and HC (Figure 2a, bottom panel). Regions with increased activation include the thalamus, S1, S2, ACC, posterior cingulate cortex (PCC), and insula. A whole-brain analysis comparing both groups showed no significant differences in laser evoked activations. Patients' laser-evoked activation maps are organized in the order of dermatomes affected as seen in Figure S1.

Our next analysis step used a region-of-interest approach to focus on S1 (Figure 2b, left panel). A two-way ANOVA showed strong evidence for a main effect of within-factor HEMISPHERE (contralateral S1 vs. ipsilateral S1, $F[1,34]) = 22.213$, $p < .001$, $\eta_p^2 = 0.417$) but no evidence for a main effect of GROUP (PHN patients vs. HC, $F[1,34]) = 0.597$, $p < .446$, $\eta_p^2 = 0.019$). There was a significant but weak evidence for an interaction between both factors ($F[1,34]) = 5.060$, $p = .032$, $\eta_p^2 = 0.140$, Figure 2b, right panel). Post-hoc paired samples t-test revealed that HC showed a clear side difference in S1 response to laser stimuli with a more pronounced response in contralateral S1 ($t = 2.523$, $p = .021$). This side difference was absent in PHN patients ($t = 0.024$, $p = .981$). Importantly, patients exhibited significantly stronger activation in ipsilateral S1 compared with HC ($t = 2.077$, $p = .045$), while contralateral S1 responses were not significantly different between the two groups ($t = 0.006$, $p = .991$).

3.4 | S1 responses related to pain perception

To test whether brain activity following laser stimulation were related to pain perception, the whole brain analysis was repeated but this time individual pain intensity ratings were included as regressors to determine their relationships to brain activity. Results showed that BOLD activity in contralateral S1 scaled with the reported pain intensity in HC. As shown in Figure 3a, the pain encoded region of S1 is closer to the upper layers, which we defined as superior S1 (SS1). In contrast, PHN patients showed pain intensity related activation in more lower layers of S1 in both hemispheres (Figure 3b), which we defined as inferior part of S1 (IS1). In addition, we also examined brain responses associated with spontaneous pain in PHN patients, as assessed by the SF-MPQ. Results showed spontaneous pain intensity related activation in the right SS1 (Figure 3a, third panel). Figure 3a (fourth panel) displays all four findings superimposed on the S1 anatomical template (yellow) for illustration purposes. Of note, there was no overlap between the cluster in contralateral SS1 identified in HC and the bilateral IS1 activation identified in PHN patients. Based on visual inspection, $z = 56$ was set as the demarcation line between activations observed in the two groups (i.e., the demarcation between IS1 and SS1). Importantly, the cluster in the right SS1 encoding spontaneous pain in PHN patients (shown in purple) strongly overlapped with the cluster in contralateral SS1 processing laser-evoked pain in HC (shown in green). This suggests that contralateral SS1 as the S1 subdivision responsible for encoding acute, evoked pain in HC becomes involved in processing spontaneous pain in PHN patients, whereas acute nociceptive stimuli engage bilateral IS1 instead. Figure 3b shows the correlation between individual pain intensity ratings and cerebral responses in S1 for illustration purposes.

3.5 | Resting-state functional connectivity between bilateral S1

Intrinsic resting-state functional connectivity between (i) left and right IS1 and (ii) left and right SS1 was compared between PHN patients and HC. Results indicated that functional connectivity between

TABLE 1 Comparison of demographic, pain, and psychological characteristics between PHN patients and healthy controls (HC, mean ± SD)

	PHN patients	Healthy controls	χ^2/t value	*p* value
Female/male	11/5	12/8	0.295	.587
Age, yr	65.75 ± 6.99	61.55 ± 8.21	1.627	.113
Education, yr	11.25 ± 3.92	12.20 ± 2.58	−0.834	.389
PRI	15.22 ± 9.19	0.90 ± 1.97	6.794	<.001
PPI	3.06 ± 1.28	0.40 ± 0.94	7.190	<.001
VAS	5.06 ± 2.30	0.55 ± 1.13	7.697	<.001
SF-MPQ	23.46 ± 12.06	1.85 ± 3.77	7.586	<.001
BDI	6.27 ± 3.93	2.15 ± 2.45	3.803	<.001
SAI	41.73 ± 13.35	26.25 ± 4.98	4.781	<.001
TAI	42.27 ± 8.48	31.05 ± 6.36	4.747	<.001

Abbreviations: BDI, Beck-Depression Index; PPI, present pain intensity; PRI, pain rating index; SAI, state-anxiety index; SF-MPQ, short-form McGill pain questionnaire; TAI, trait-anxiety index; VAS, 10-cm visual analogue scale.

bilateral IS1 was not significantly different between PHN patients and HC ($t = 0.886$, $p = .381$), and was not correlated with spontaneous pain in PHN patients ($r = -.171$, $p = .942$, Figure 4a). In contrast, PHN patients exhibited significantly weaker functional connectivity between bilateral SS1 than HC ($t = 2.355$, $p = .024$). Importantly, this bilateral SS1 functional connectivity was negatively correlated with spontaneous pain in PHN patients ($r = -.526$, $p = .036$, Figure 4b). That is, the more intense the spontaneous pain, the less intrinsic resting-state functional connectivity we found between left and right SS1. Results for the control region (i.e., M1) showed that functional connectivity between bilateral M1 was not significantly different between PHN patients and HC ($t = 0.731$, $p = .470$) and was not correlated with spontaneous pain in PHN patients ($r = -.138$, $p = .610$, Figure 4c).

3.6 | S1 activity predicts spontaneous and evoked pain intensities

Using a multivariate pattern analysis approach, we first tested whether pain ratings could be predicted from structural brain measures. When gray matter volume in IS1 was used as predictor, prediction of HC's intensity ratings of evoked pain was not successful ($r = .237$, $p = .315$; Figure 5A[a]). Likewise, gray matter volume of IS1 could not predict laser-evoked pain ratings or SF-MPQ ratings in PHN patients ($r = .190$, $p = .481$; $r = .043$, $p = .874$; Figure 5B[b,c]). A similar pattern was found for predictions from SS1 gray matter volume. Prediction of HC's intensity ratings of evoked pain was not successful ($r = .172$, $p = .468$; Figure 5A[d]) and in PHN patients, SS1 gray matter volume did not predict laser-evoked pain ratings and SF-MPQ ratings ($r = .014$, $p = .095$; $r = .021$, $p = .939$; Figure 5A[e,f]).

Turning to predictions from functional brain measures, we found that IS1 activity in HC was unable to predict their ratings of laser-evoked pain ($r = .052$, $p = .829$; Figure 5B[a]), whereas in PHN patients, IS1 activity predicted ratings of evoked pain ($r = .566$, $p = .024$; Figure 5B[b]), but not of spontaneous pain (assessed by SF-MPQ; $r = .235$, $p = .379$; Figure 5B[c]). When BOLD activity in SS1 was used as a predictor, SS1 activity in HC was able to predict their ratings of laser-evoked pain ($r = .509$, $p = .022$; Figure 5B[d]). In contrast, SS1 activity in PHN patients was unable to predict ratings of evoked pain ($r = .267$, $p = .317$; Figure 5B[e]), but could predict spontaneous pain (assessed by SF-MPQ; $r = .469$, $p = .050$; Figure 5B[f]).

Finally, using resting-state functional connectivity data, ratings of spontaneous pain in PHN patients were unable to predicted by bilateral IS1 functional connectivity ($r = .082$, $p = .761$; Figure 5C[a]), but could predicted by bilateral SS1 functional connectivity ($r = .519$, $p = .039$; Figure 5C [b]). In contrast, ratings of evoked pain in HC could not be predicted by resting-state functional connectivity of bilateral SS1 and bilateral IS1.

4 | DISCUSSION

S1 is known to be a key brain region for pain processing. Changes in S1 activity and functional organization have so far mainly been documented for patients with PLP, CRPS, and SCI. Here, we investigated whether structural and functional alterations can also be found in patients suffering from PHN. As the main finding of this study, we report functional S1 reorganization in PHN patients related to acute evoked as well as spontaneous pain. Following laser stimulation, PHN patients did not show the typical lateralized contralateral S1 response but instead displayed bilateral activation and significantly stronger ipsilateral S1 activity than controls. More specifically, the laser stimulation engaged the (bilateral) inferior sections of S1 (IS1), whereas activity was located in a superior (contralateral) section of S1 in HC. Importantly, the right superior portion of S1 (SS1) that responded to (contralateral) stimulation in HC, encoded spontaneous pain (SF-MPQ) in PHN patients. Resting-state fMRI data showed weaker bilateral SS1 functional connectivity in PHN patients than in HC, and the degree of functional connectivity was negatively correlated with spontaneous pain (SF-MPQ). Lastly, using MVPA, we found that BOLD activity in S1 subregions predicted intensity ratings of laser and

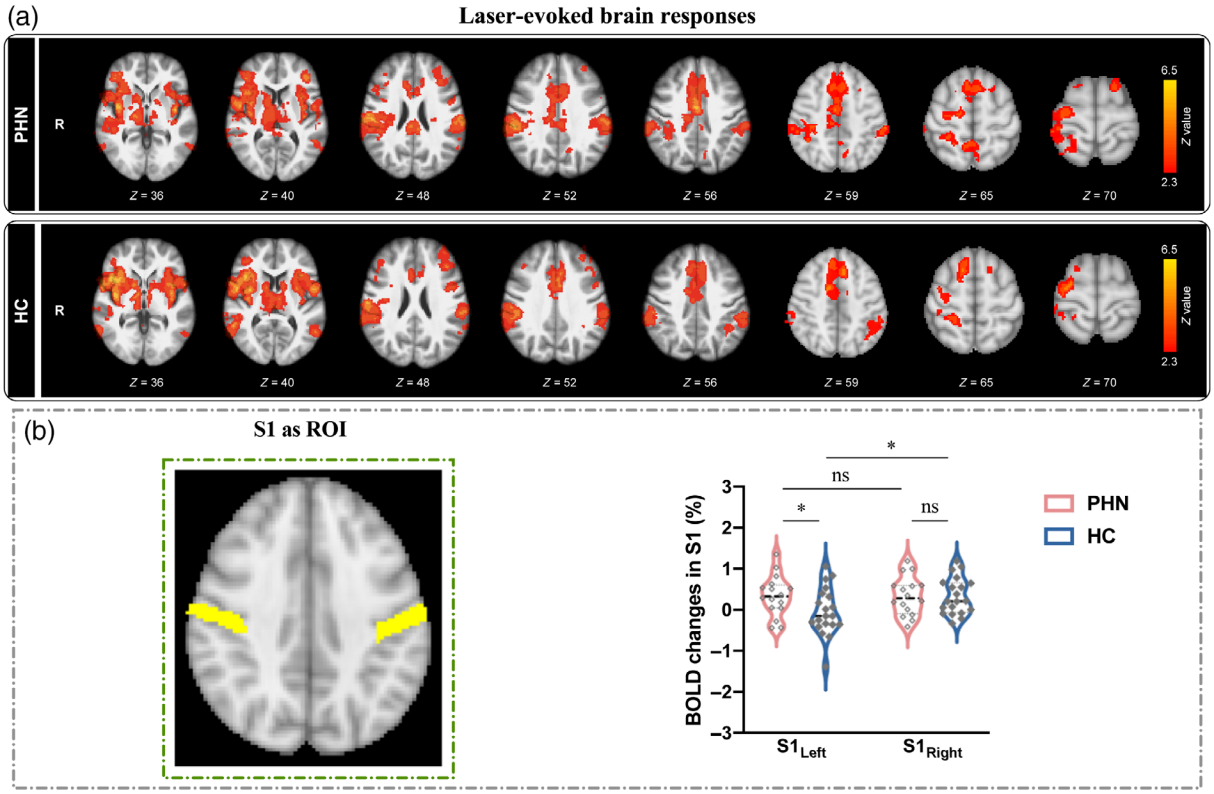

FIGURE 2 BOLD activations in response to nociceptive laser stimuli in S1. (a) Nociceptive laser stimuli elicited significant activations in the primary/secondary somatosensory cortices (S1/S2), thalamus, anterior cingulate cortex (ACC), posterior cingulate cortex (PCC), and insula in both PHN patients (top panel) and HC (bottom panel). (b) The comparison of BOLD percentage changes in bilateral S1. When the bilateral S1 (MNI anatomical template) were used as the ROIs, two-way ANOVA analysis revealed that HC exhibited a significant activation focus in contralateral S1 to the stimulated (left) hand; while PHN patients showed greater activation in ipsilateral S1 than HC (ns, not significant; *$p < .05$).

spontaneous pain in PHN patients and HC, and resting-state functional connectivity between left and right SS1 was able to predict the intensity of spontaneous pain in PHN patients.

4.1 | Laser-evoked brain activity in S1

The comparison of laser-evoked BOLD activity showed that the noxious stimulation engaged S1 in both hemispheres in PHN patients with more pronounced ipsilateral S1 activity than in HC. Given that afferent somatosensory fibers decussate at the level of the spinal cord, a signal increase in contralateral S1 is expected and has been demonstrated in a multitude of imaging studies in healthy individuals using electrical stimulation, vibration, and touch as stimuli (Kropf et al., 2019). In contrast, ipsilateral activation is less frequent. A signal increase in ipsilateral S1 most likely reflects input from contralateral S1—either through direct transcallosal connections (Allison et al., 1989) or through projections via the S2 or thalamus (Blankenburg et al., 2008). This also explains the later onset of ipsilateral compared with contralateral activation in intracranial and MEG recordings (Allison et al., 1989; Kanno et al., 2003). Plasticity studies in animals and humans have demonstrated increased ipsilateral S1 responses, for instance, following peripheral nerve deafferentation or stroke, suggesting that they can be part of a clinical syndrome indicating CNS pathology (Lindberg et al., 2007; Pelled et al., 2007).

4.2 | Different encoding patterns of evoked and spontaneous pain in S1

In order to directly link our findings to pain perception, we tested whether activity in S1 scaled with patients' pain intensity ratings. Similar to the group of healthy volunteers, PHN patients showed pain-related activity in S1 albeit with a markedly different topography. Healthy controls exhibited a stimulation-induced increase in signal level that correlated with reported pain intensity in contralateral S1. In the patient group, the same analysis revealed significant bilateral S1 activity with more pronounced activity in the inferior section of S1 (IS1) on the contralateral side compared with controls. Pain that occurred spontaneously in these patients on the other hand engaged the right superior portion of S1 (SS1) that processed acute noxious stimuli in healthy controls. Together, these findings suggest S1 functional reorganization in those with PHN.

Because our study protocol did not include extensive mapping of different body parts beyond the noxious stimulation that was applied to an unaffected site (e.g., dorsal aspect of the left hand), we can only speculate about potential reasons for this reorganization. In most

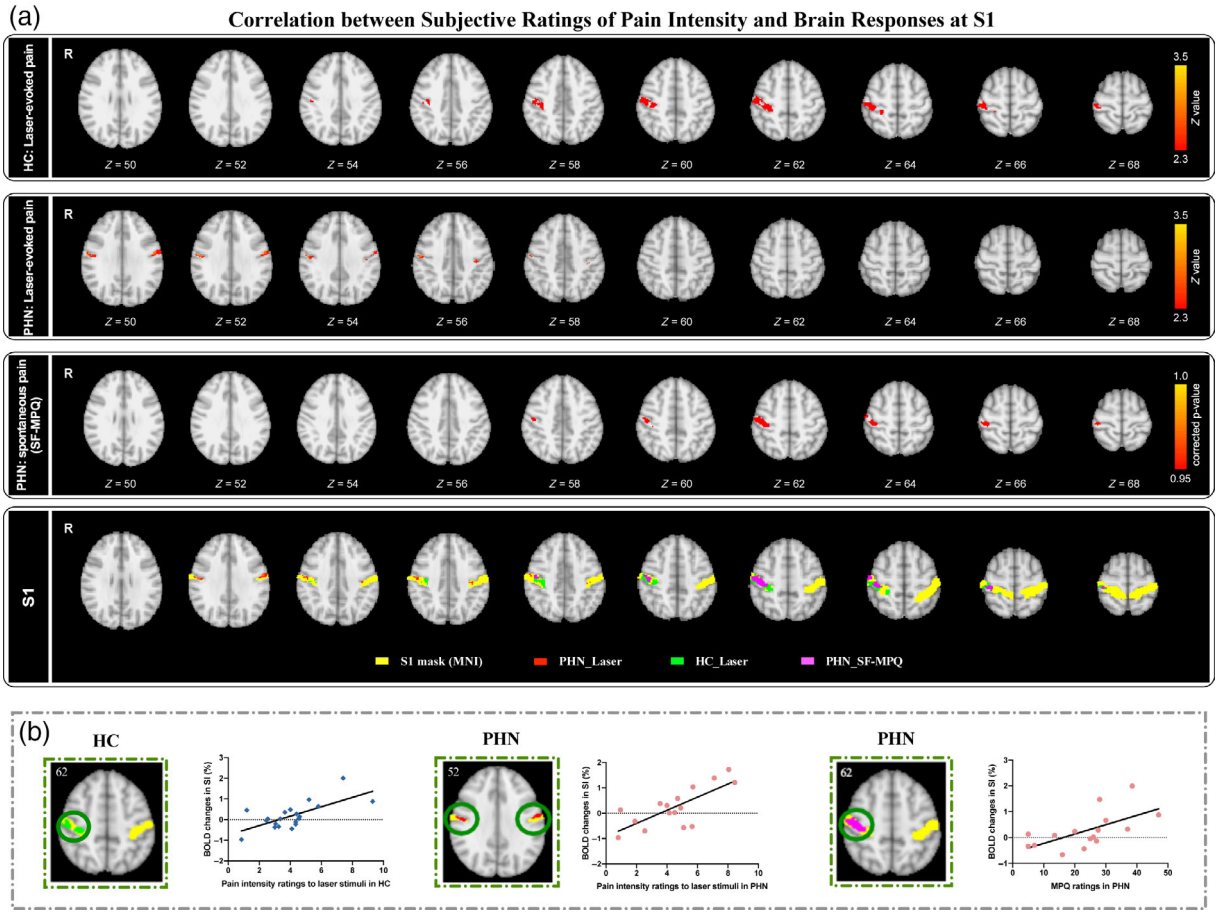

FIGURE 3 Correlation between pain intensity ratings and S1 responses to laser stimulation. (a) S1 activity maps reflecting subjective ratings of laser-evoked and spontaneous pain. Subjective ratings of laser-evoked pain were positively correlated with activations of contralateral SS1 in HC (first panel). Subjective ratings of laser-evoked pain were positively correlated with activations of bilateral IS1 in PHN patients (second panel). Subjective ratings of spontaneous pain assessed by SF-MPQ were positively correlated with activations of the right SSI in PHN patients (third panel). Positive brain activity maps of both groups were superimposed on the S1 anatomical template (fourth panel). Yellow mark, S1 anatomical template; green mark, positive brain activity map identified by subjective ratings of laser-evoked pain in HC; red mark, positive brain activity map identified by subjective ratings of laser-evoked pain in PHN patients; purple mask, positive brain activity map identified by subjective ratings of spontaneous pain in PHN patients. (b) Scatter plots show the correlations between subjective ratings of pain and responses in S1.

patients of our study, PHN-related pain was located on the right side of the trunk and right wrist. According to the S1 homunculus, both these sites are represented more superiorly than the hand where the noxious laser stimuli were applied. While this relative placement was preserved, both representations seem to have shifted toward a more inferior position in the patient group compared with the healthy controls. This observation is compatible with the notion of an enlarged representation of the affected body parts and a shift of the finger representation toward a more inferior position. So far, studies investigating S1 reorganization in the context of chronic pain have largely reported reduced representation of the affected body part (although see (Mancini et al., 2019). However, these observations predominantly stem from patient groups in which the hurting body part is no longer present (e.g., PLP), is deafferented (e.g., following SCI) or in which pain has largely led to the disuse of the affected extremity (e.g., CRPS). With afferent pathways' generally intact and nociceptive input increased, PHN patients in contrast might rather show changes in S1 organization that are known from scenarios with increased afferent input (e.g., somatosensory training). In this case, body parts that received stimulation would show an enlarged representation in S1. In our case, this would mean an enlarged representation of the sites of spontaneous pain (e.g., trunk and wrist) including the part of S1 that would normally respond to input from the fingers. As a consequence of this expansion, body parts situated below (e.g., fingers) would now engage a more inferior section in the homunculus compared with the representation in healthy controls. Whether such "training-like" effects indeed add to the organizational pattern found in our study remains to be investigated.

4.3 | Resting-state functional connectivity between bilateral S1

Our analysis of resting-state functional connectivity revealed that the intrinsic connectivity between bilateral SS1 was significantly weaker in PHN patients than in HC, and that the connectivity

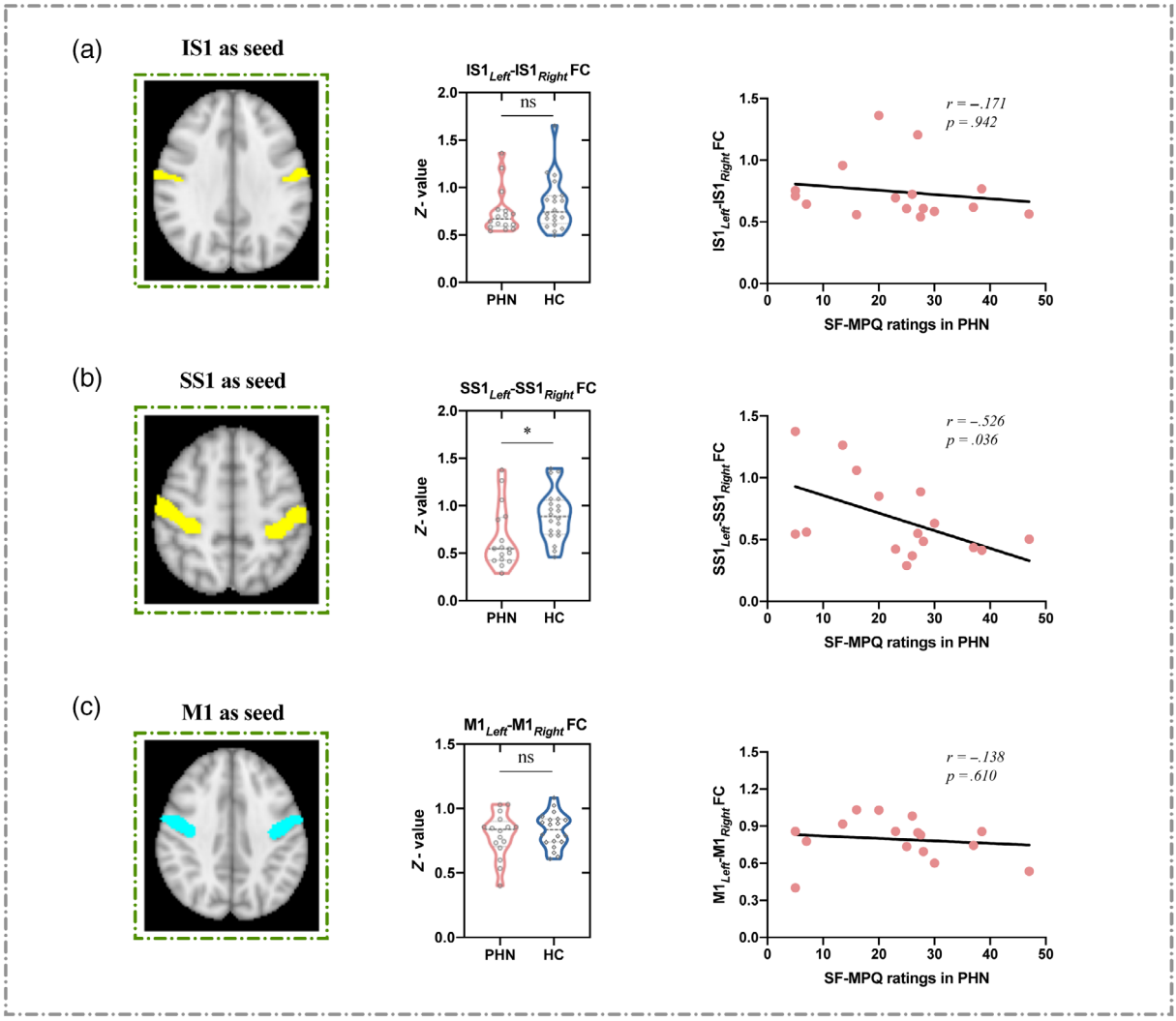

FIGURE 4 Resting-state functional connectivity (FC) in bilateral IS1/SS1/M1. (a) When IS1 was used as the seed, resting-state FC in bilateral IS1 was not significantly different between PHN patients and HC (ns, no significant; middle panel); resting-state FC in bilateral IS1 was not correlated with SF-MPQ ratings in PHN patients (right panel). (b) When SS1 was used as the seed, PHN patients exhibited weaker resting-state FC in bilateral SS1 than HC (*$p < .05$; middle panel); resting-state FC in bilateral SS1 was negatively correlated with SF-MPQ ratings in PHN patients (right panel). (c) When M1 was used as the seed, resting-state FC between left and right M1 was not significantly different between PHN patients and HC (ns, no significant; middle panel); resting-state FC in bilateral M1 was not correlated with SF-MPQ ratings in PHN patients (right panel).

between both regions was negatively correlated with spontaneous pain. Of note, such reduced functional connectivity was not found in the adjacent M1.

A study by Tal et al. recently identified two relevant features of resting-state connectivity between left and right S1 in healthy individuals (Tal et al., 2017). Firstly, connectivity follows the same somatotopic organization as activations depicted in the homunculus and secondly, connections between hemispheres are strongest between homologous regions and with decreasing connectivity to adjacent body parts. This gradient has been interpreted as a sharpening mechanism that ensures optimal information processing in homologue regions. Our findings showed that it is not only the representation of peripheral input and spontaneous pain that is disrupted but also the connectivity with the ipsilateral homologue and that this alteration scales with the pain intensity reported.

So far, the link between S1 connectivity and pain perception is only poorly understood, and findings are inconsistent. For instance, Kong et al. reported reduced functional connectivity between left and right S1 in chronic low back pain patients, with bilateral S1 functional connectivity positively predicting the intensity of low back pain (Kong et al., 2013). Furthermore, changes can also occur in the connectivity between S1 and other brain regions. Our recent work in PHN patients found enhanced functional connectivity between right S1 and thalamus as well as decreased functional connectivity between left S1 and PAG, which was correlated with increased pain intensities at resting state (Li et al., 2020).

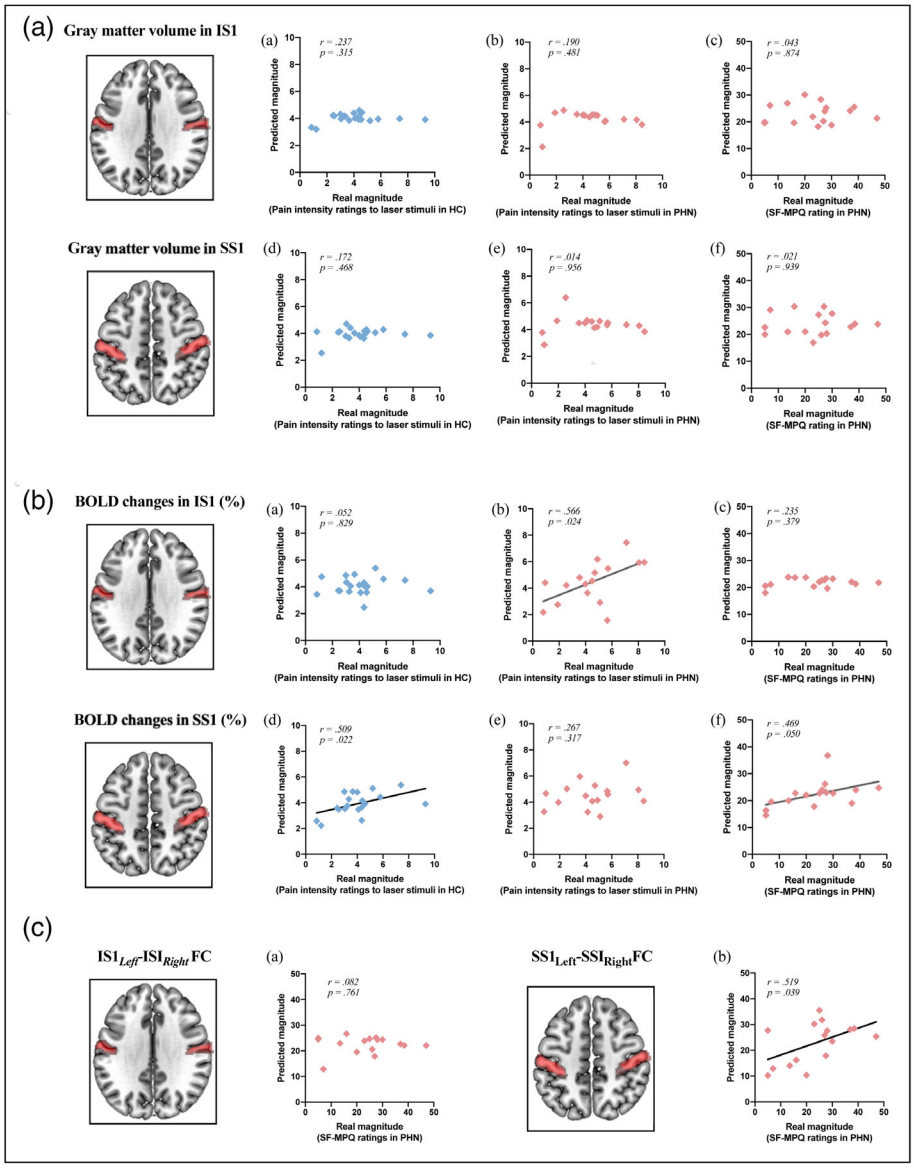

FIGURE 5 Prediction of subjective intensities of evoked and spontaneous pain using S1 features. (A) When gray matter volume in IS1 was used as predictors, gray matter volume of IS1 in HC could not predict laser-evoked pain ratings across HC (a), and gray matter volume of IS1 in PHN patients could not predict laser-evoked pain ratings and SF-MPQ ratings across patients (b,c); when gray matter volume in SS1 was used as predictors, gray matter volume of SS1 in HC could not predict laser-evoked pain ratings across HC (d), and gray matter volume of SS1 in PHN patients could not predict laser-evoked pain ratings and SF-MPQ ratings across patients (e,f). (B) When BOLD activity in IS1 was used as predictors, IS1 activity in HC could not predict laser-evoked pain ratings across HC (a); however, IS1 activity in PHN patients could predict laser-evoked pain ratings (b) but not SF-MPQ ratings (c); when BOLD activity in SS1 was used as predictors, SS1 activity in HC was able to predict laser-evoked pain ratings across HC (a); and SS1 activity in PHN patients was unable to predict laser-evoked pain ratings (b), but able to predict SF-MPQ ratings across patients (c). (C) PHN patients' FC of bilateral IS1 was unable to predict SF-MPQ ratings across patients (a); PHN patients' FC of bilateral SS1 was able to predict SF-MPQ ratings across patients (b).

4.4 | Prediction of within-subject variability of pain intensity from S1 features

As a final step in our series of analyses, we formally tested whether structural and functional features of IS1 and SS1 could predict within-subject variability of pain intensity. To this end, we used a multivariate pattern analysis approach to decode within-subject variability of pain intensity associated with spontaneous and laser-evoked pain from S1 gray matter volume, activity related to evoked and spontaneous pain as well as resting-state functional connectivity. Findings of previous investigations into structural and functional changes in S1 in several chronic pain conditions have been controversial as they reported increases, decreases, or no change in S1 activity (Klug et al., 2011; Lenz et al., 1987). We found that laser-evoked pain was predicted by IS1 activity in PHN patients and by SS1 activity in controls, whereas SS1 activity predicted spontaneous pain in patients. These observations confirm our univariate analyses and suggest that changes in S1 could potentially function as predictors for inter-individual differences for pain perception. Further investigations are needed to specify neural processes underlying these alterations. Possible routes to this reorganization include an increase in bottom-up information transfer (e.g., through increased peripheral input) and a decrease of top-down modulation that reveals a reorganized S1 map.

5 | CONCLUSION AND OUTLOOK

Together, our findings provide robust evidence for changes in functional features of S1 in patients with PHN-related pain. However, they also raise a number of questions that need to be addressed. Firstly, we only applied nociceptive stimuli to the participants' left hand, which limits our ability to explore the lateralization of responses. Further studies are therefore needed to investigate any site-specific differences. Secondly, the MVPA results were not

validated in a separate dataset which should be the focus of future investigations. Thirdly, it needs to be explored what led to the functional reorganization, why patients show a predominantly ipsilateral response and whether alterations in S1 representation are a cause or consequence of changes in functional connectivity. Only longitudinal studies in larger samples allow us to track the development of the key variables over time to shed light on their relationship and develop a causal model of plasticity underlying pain perception and neural processing in PHN. Finally, the correlation between changes in S1 functional organization and pain (evoked and spontaneous) requires further investigation. The relationship between these two variables has been debated in the context of PLP for a long time but it has remained unclear how changes in the representation or connectivity of S1 can give rise to the sensation of pain.

CONFLICT OF INTEREST

All authors declare no conflict of interest.

DATA AVAILABILITY STATEMENT

The data and codes that support the findings of this study are available from the corresponding author upon reasonable request. The data are not publicly available due to privacy or ethical restrictions.

ORCID

Hong Li https://orcid.org/0000-0003-2810-1914
Yazhuo Kong https://orcid.org/0000-0002-8249-4723

REFERENCES

Allison, T., McCarthy, G., Wood, C. C., Darcey, T. M., Spencer, D. D., & Williamson, P. D. (1989). Human cortical potentials evoked by stimulation of the median nerve. I. Cytoarchitectonic areas generating short-latency activity. *Journal of Neurophysiology*, *62*(3), 694–710.

Apkarian, A. V., Bushnell, M. C., Treede, R. D., & Zubieta, J. K. (2005). Human brain mechanisms of pain perception and regulation in health and disease. *European Journal of Pain*, *9*(4), 463–484.

Beck, A. T., Steer, R. A., Ball, R., & Ranieri, W. F. (1996). Comparison of Beck depression inventories-IA and -II in psychiatric outpatients. *Journal of Personality Assessment*, *67*(3), 588–597.

Beckmann, C. F., Jenkinson, M., & Smith, S. M. (2003). General multilevel linear modeling for group analysis in FMRI. *NeuroImage*, *20*(2), 1052–1063.

Beckmann, C. F., & Smith, S. M. (2004). Probabilistic independent component analysis for functional magnetic resonance imaging. *IEEE Transactions on Medical Imaging*, *23*(2), 137–152.

Bjorkman, A., Weibull, A., Olsrud, J., Ehrsson, H. H., Rosen, B., & Bjorkman-Burtscher, I. M. (2012). Phantom digit somatotopy: A functional magnetic resonance imaging study in forearm amputees. *The European Journal of Neuroscience*, *36*(1), 2098–2106.

Blankenburg, F., Ruff, C. C., Bestmann, S., Bjoertomt, O., Eshel, N., Josephs, O., Weiskopf, N., & Driver, J. (2008). Interhemispheric effect of parietal TMS on somatosensory response confirmed directly with concurrent TMS-fMRI. *The Journal of Neuroscience*, *28*(49), 13202–13208.

Bromm, B., & Treede, R. D. (1984). Nerve-fiber discharges, cerebral potentials and sensations induced by CO_2-laser stimulation. *Human Neurobiology*, *3*(1), 33–40.

Desbordes, G., Li, A., Loggia, M. L., Kim, J., Schalock, P. C., Lerner, E., Tran, T. N., Ring, J., Rosen, B. R., Kaptchuk, T. J., Pfab, F., & Napadow, V. (2015). Evoked itch perception is associated with changes in functional brain connectivity. *NeuroImage: Clinical*, *7*, 213–221.

Doehrmann, O., Ghosh, S. S., Polli, F. E., Reynolds, G. O., Horn, F., Keshavan, A., Triantafyllou, C., Saygin, Z. M., Whitfield-Gabrieli, S., Hofmann, S. G., Pollack, M., & Gabrieli, J. D. (2013). Predicting treatment response in social anxiety disorder from functional magnetic resonance imaging. *JAMA Psychiatry*, *70*(1), 87–97.

Dworkin, R. H. (2002). An overview of neuropathic pain: Syndromes, symptoms, signs, and several mechanisms. *Clinical Journal of Pain*, *18*(6), 343–349.

Endo, T., Spenger, C., Hao, J., Tominaga, T., Wiesenfeld-Hallin, Z., Olson, L., & Xu, X. J. (2008). Functional MRI of the brain detects neuropathic pain in experimental spinal cord injury. *Pain*, *138*(2), 292–300.

Fields, H. L., Rowbotham, M., & Baron, R. (1998). Postherpetic neuralgia: Irritable nociceptors and deafferentation. *Neurobiology of Disease*, *5*(4), 209–227.

Flor, H., Elbert, T., Knecht, S., Wienbruch, C., Pantev, C., Birbaumers, N., Larbig, W., & Taub, E. (1995). Phantom-limb pain as a perceptual correlate of cortical reorganization following arm amputation. *Nature*, *375*(6531), 482–484.

Freund, P., Weiskopf, N., Ward, N. S., Hutton, C., Gall, A., Ciccarelli, O., Craggs, M., Friston, K., & Thompson, A. J. (2011). Disability, atrophy and cortical reorganization following spinal cord injury. *Brain*, *134*(Pt 6), 1610–1622.

Geha, P. Y., Baliki, M. N., Chiaivo, D. R., Harden, R. N., Paice, J. A., & Apkarian, A. V. (2007). Brain activity for spontaneous pain of postherpetic neuralgia and its modulation by lidocaine patch therapy. *Pain*, *128*(1-2), 88–100.

Grabher, P., Callaghan, M. F., Ashburner, J., Weiskopf, N., Thompson, A. J., Curt, A., & Freund, P. (2015). Tracking sensory system atrophy and outcome prediction in spinal cord injury. *Annals of Neurology*, *78*(5), 751–761.

Hu, L., Zhang, L., Chen, R., Yu, H., Li, H., & Mouraux, A. (2015). The primary somatosensory cortex and the insula contribute differently to the processing of transient and sustained nociceptive and non-nociceptive somatosensory inputs. *Human Brain Mapping*, *36*(11), 4346–4360.

Jenkinson, M., Bannister, P., Brady, M., & Smith, S. (2002). Improved optimization for the robust and accurate linear registration and motion correction of brain images. *NeuroImage*, *17*(2), 825–841.

Jin, Q. Q., Wu, G. Q., Peng, W. W., Xia, X. L., Hu, L., & Iannetti, G. D. (2018). Somatotopic representation of second pain in the primary somatosensory cortex of humans and rodents. *Journal of Neuroscience*, *38*(24), 5538–5550.

Juottonen, K., Gockel, M., Silen, T., Hurri, H., Hari, R., & Forss, N. (2002). Altered central sensorimotor processing in patients with complex regional pain syndrome. *Pain*, *98*(3), 315–323.

Kambi, N., Halder, P., Rajan, R., Arora, V., Chand, P., Arora, M., & Jain, N. (2014). Large-scale reorganization of the somatosensory cortex following spinal cord injuries is due to brainstem plasticity. *Nature Communications*, *5*, 3602.

Kanno, A., Nakasato, N., Hatanaka, K., & Yoshimoto, T. (2003). Ipsilateral area 3b responses to median nerve somatosensory stimulation. *NeuroImage*, *18*(1), 169–177.

Klug, S., Anderer, P., Saletu-Zyhlarz, G., Freidl, M., Saletu, B., Prause, W., & Aigner, M. (2011). Dysfunctional pain modulation in somatoform pain disorder patients. *European Archives of Psychiatry and Clinical Neuroscience*, *261*(4), 267–275.

Kong, J., Spaeth, R. B., Wey, H. Y., Cheetham, A., Cook, A. H., Jensen, K., Tan, Y., Liu, H. S., Wang, D. H., Loggia, M. L., Napadow, V., Smoller, J. W., Wasan, A. D., & Gollub, R. L. (2013). S1 is associated with chronic low back pain: A functional and structural MRI study. *Molecular Pain*, *9*, 43.

Kropf, E., Syan, S. K., Minuzzi, L., & Frey, B. N. (2019). From anatomy to function: The role of the somatosensory cortex in emotional regulation. *Brazilian Journal of Psychiatry*, *41*(3), 261–269.

Lenz, F. A., Tasker, R. R., Dostrovsky, J. O., Kwan, H. C., Gorecki, J., Hirayama, T., & Murphy, J. T. (1987). Abnormal single-unit activity recorded in the somatosensory thalamus of a quadriplegic patient with central pain. *Pain*, *31*(2), 225–236.

Li, H., Li, X., Feng, Y., Gao, F., Kong, Y., & Hu, L. (2020). Deficits in ascending and descending pain modulation pathways in patients with postherpetic neuralgia. *NeuroImage*, *221*, 117186.

Li, M., Yan, J., Li, S., Wang, T., Zhan, W., Wen, H., Ma, X., Zhang, Y., Tian, J., & Jiang, G. (2017). Reduced volume of gray matter in patients with trigeminal neuralgia. *Brain Imaging and Behavior*, *11*(2), 486–492.

Lindberg, P. G., Schmitz, C., Engardt, M., Forssberg, H., & Borg, J. (2007). Use-dependent up- and down-regulation of sensorimotor brain circuits in stroke patients. *Neurorehabilitation and Neural Repair*, *21*(4), 315–326.

Lindquist, M. A., Krishnan, A., Lopez-Sola, M., Jepma, M., Woo, C. W., Koban, L., Roy, M., Atlas, L. Y., Schmidt, L., Chang, L. J., Reynolds Losin, E. A., Eisenbarth, H., Ashar, Y. K., Delk, E., & Wager, T. D. (2017). Group-regularized individual prediction: Theory and application to pain. *NeuroImage*, *145*(Pt B), 274–287.

Liu, J., Hao, Y., Du, M., Wang, X., Zhang, J., Manor, B., Jiang, X., Fang, W., & Wang, D. (2013). Quantitative cerebral blood flow mapping and functional connectivity of postherpetic neuralgia pain: A perfusion fMRI study. *Pain*, *154*(1), 110–118.

Liu, P., Wang, G., Liu, Y., Zeng, F., Lin, D., Yang, X., Liang, F., Calhoun, V. D., & Qin, W. (2017). Disrupted intrinsic connectivity of the periaqueductal gray in patients with functional dyspepsia: A resting-state fMRI study. *Neurogastroenterology and Motility*, *29*(8), e13060.

Luerding, R., Weigand, T., Bogdahn, U., & Schmidt-Wilcke, T. (2008). Working memory performance is correlated with local brain morphology in the medial frontal and anterior cingulate cortex in fibromyalgia patients: Structural correlates of pain-cognition interaction. *Brain*, *131*(Pt 12), 3222–3231.

Maihofner, C., Handwerker, H. O., Neundorfer, B., & Birklein, F. (2003). Patterns of cortical reorganization in complex regional pain syndrome. *Neurology*, *61*(12), 1707–1715.

Makin, T. R., Scholz, J., Filippini, N., Henderson Slater, D., Tracey, I., & Johansen-Berg, H. (2013). Phantom pain is associated with preserved structure and function in the former hand area. *Nature Communications*, *4*(1), 1–8.

Mancini, F., Wang, A. P., Schira, M. M., Isherwood, Z. J., McAuley, J. H., Iannetti, G. D., Sereno, M. I., Moseley, G. L., & Rae, C. D. (2019). Fine-grained mapping of cortical somatotopies in chronic complex regional pain syndrome. *The Journal of Neuroscience*, *39*(46), 9185–9196.

May, A. (2011). Structural brain imaging: A window into chronic pain. *The Neuroscientist*, *17*, 209–220.

Melzack, R. (1987). The short-form McGill pain questionnaire. *Pain*, *30*(2), 191–197.

Obermann, M., Rodriguez-Raecke, R., Naegel, S., Holle, D., Mueller, D., Yoon, M. S., Theysohn, N., Blex, S., Diener, H. C., & Katsarava, Z. (2013). Gray matter volume reduction reflects chronic pain in trigeminal neuralgia. *NeuroImage*, *74*, 352–358.

Pelled, G., Chuang, K. H., Dodd, S. J., & Koretsky, A. P. (2007). Functional MRI detection of bilateral cortical reorganization in the rodent brain following peripheral nerve deafferentation. *NeuroImage*, *37*(1), 262–273.

Price, D. D. (2000). Neuroscience - psychological and neural mechanisms of the affective dimension of pain. *Science*, *288*(5472), 1769–1772.

Sah, D. W. Y., Ossipov, M. H., & Porreca, F. (2003). Neurotrophic factors as novel therapeutics for neuropathic pain. *Nature Reviews Drug Discovery*, *2*(6), 460–472.

Scholz, J., Finnerup, N. B., Attal, N., Aziz, Q., Baron, R., Bennett, M. I., Benoliel, R., Cohen, M., Cruccu, G., Davis, K. D., Evers, S., First, M., Giamberardino, M. A., Hansson, P., Kaasa, S., Korwisi, B., Kosek, E., Lavand'homme, P., Nicholas, M., … NeuPSIG. (2019). The IASP classification of chronic pain for ICD-11: Chronic neuropathic pain. *Pain*, *160*(1), 53–59.

Seifert, F., & Maihofner, C. (2009). Central mechanisms of experimental and chronic neuropathic pain: Findings from functional imaging studies. *Cellular and Molecular Life Sciences*, *66*(3), 375–390.

Smith, S. M., Zhang, Y. Y., Jenkinson, M., Chen, J., Matthews, P. M., Federico, A., & De Stefano, N. (2002). Accurate, robust, and automated longitudinal and cross-sectional brain change analysis. *NeuroImage*, *17*(1), 479–489.

Tal, Z., Geva, R., & Amedi, A. (2017). Positive and negative somatotopic BOLD responses in contralateral versus ipsilateral Penfield homunculus. *Cerebral Cortex*, *27*(2), 962–980.

Tu, Y., Jung, M., Gollub, R. L., Napadow, V., Gerber, J., Ortiz, A., Lang, C., Mawla, I., Shen, W., Chan, S. T., Wasan, A. D., Edwards, R. R., Kaptchuk, T. J., Rosen, B., & Kong, J. (2019). Abnormal medial prefrontal cortex functional connectivity and its association with clinical symptoms in chronic low back pain. *Pain*, *160*(6), 1308–1318.

Valentini, E., Hu, L., Chakrabarti, B., Hu, Y., Aglioti, S. M., & Iannetti, G. D. (2012). The primary somatosensory cortex largely contributes to the early part of the cortical response elicited by nociceptive stimuli. *NeuroImage*, *59*(2), 1571–1581.

Wager, T. D., Atlas, L. Y., Leotti, L. A., & Rilling, J. K. (2011). Predicting individual differences in placebo analgesia: Contributions of brain activity during anticipation and pain experience. *The Journal of Neuroscience*, *31*(2), 439–452.

Woolrich, M. W., Behrens, T. E. J., Beckmann, C. F., Jenkinson, M., & Smith, S. M. (2004). Multilevel linear modelling for FMRI group analysis using Bayesian inference. *NeuroImage*, *21*(4), 1732–1747.

Woolrich, M. W., Ripley, B. D., Brady, M., & Smith, S. M. (2001). Temporal autocorrelation in univariate linear modeling of FMRI data. *NeuroImage*, *14*(6), 1370–1386.

SUPPORTING INFORMATION

Additional supporting information can be found online in the Supporting Information section at the end of this article.

How to cite this article: Li, H., Li, X., Wang, J., Gao, F., Wiech, K., Hu, L., & Kong, Y. (2022). Pain-related reorganization in the primary somatosensory cortex of patients with postherpetic neuralgia. *Human Brain Mapping*, 1–13. https://doi.org/10.1002/hbm.25992